Carbohydrate Polymers 156 (2017) 409–416

Contents lists available at ScienceDirect

Carbohydrate Polymers

journal homepage: www.elsevier.com/locate/carbpol

Properties of cellulose nanocrystals from oil palm trunk isolated by total chlorine free method

Junidah Lamaming, Rokiah Hashim*, Cheu Peng Leh, Othman Sulaiman

Division of Bioresource, Paper and Coatings Technology, School of Industrial Technology, Universiti Sains Malaysia, 11800, Minden, Penang, Malaysia

ARTICLE INFO

Article history:
Received 9 April 2016
Received in revised form 9 September 2016
Accepted 15 September 2016
Available online 16 September 2016

Keywords:
Oil palm
Cellulose nanocrystals
Total chlorine free
Ozone bleaching
Water pre-hydrolysis
Crystallinity

ABSTRACT

Cellulose nanocrystals were isolated from oil palm trunk by total chlorine free method. The samples were either water pre-hydrolyzed or non-water pre-hydrolyzed, subjected to soda pulping, acidified and ozone bleached. Cellulose and cellulose nanocrystal (CNC) physical, chemical, thermal properties, and crystallinity index were investigated by composition analysis, scanning electron microscopy, transmission electron microscopy, fourier transform infrared, thermogravimetric analysis and X-ray diffraction. Water pre-hydrolysis reduced lignin (<0.5%) and increased holocellulose (99.6%) of ozone-bleached cellulose. Water pre-hydrolyzed cellulose exhibited surface fibrillation and peeling off after acid hydrolysis process compared to non-fibrillated of non-water pre-hydrolyzed cellulose. Water pre-hydrolysis improved final CNC crystallinity (up to 75%) compared to CNC without water pre-hydrolysis crystallinity (69%). Cellulose degradation was found to occur during ozone bleaching stage but CNC showed an increase in crystallinity after acid hydrolysis. Thus, oil palm trunk CNC can be potentially applied in pharmaceutical, food, medical and nanocomposites.

1. Introduction

Research on green materials from natural sources such as cellulosic materials open up a plethora applications to venture either in the manufacturing, packaging, electrical, pharmaceutical, medical industries and even in the biofuels industries (Eichhorn, 2011; Eichhorn, 2011; Habibi, Lucia, & Rojas, 2010; Lavoine, Desloges, Dufresne, & Bras, 2012; Brinchi, Cotana, Fortunati, & Kenny, 2013). One such green material is cellulose nanocrystal. It is inexpensive having a high aspect ratio, good mechanical properties, high absorbency, fully degradable, renewable resources and free of toxic (Brinchi et al., 2013). Cellulose nanocrystals garnered the attention of the researchers around the world. Ongoing research includes the isolation of the cellulose from various new natural sources, improvement of the processing methods and products, and also covered on the potential applications of the cellulose nanocrystals (Eichhorn et al., 2010; Habibi et al., 2010; Durán, Lemes, Durán, Freer, & Baeza, 2011; Lavoine et al., 2012; Brinchi et al., 2013).

The conventional process of obtaining cellulose nanocrystal involves chlorine based compounds that were used as one of the bleaching agents to increase brightness and cleanliness of the fibers. This process also removed remaining unwanted particles effectively. However, the impact of chlorinated organic compounds discharged from this process gives a harmful impact on the human health and it is also not environmentally friendly. Thus, seeking bleaching process that is less polluting known as total chlorine free (TCF) bleaching is important. This bleaching method substitutes the chlorine and chlorine-based bleaching chemicals with oxygen and oxygen based compounds such as hydrogen peroxide and ozone.

According to Shatalov & Pereira (2008), ozone is highly efficient bleaching process in terms of delignification ability. From the environmental point of view, ozone is good, however, it could cause degradation that led to a reduction of mechanical properties in pulp strength (Shatalov & Pereira, 2007). The cellulose degradation was caused by generations of the OH radicals (oxidizing species) when the ozone reacts with the phenolic rings in lignin that led to the formation of new carbonyl groups (Chandra & Gratzl, 1985; Ragnar, Eriksson, & Reitberger, 1999 Simões & Castro, 2001; Pouyet, Chirat, Potthast, & Lachenal, 2014).

Eliminating the lignin to the greatest extent is crucial before the pulps were being subjected to ozone as very few carbonyl groups are created on the cellulose-lignin free pulp. Acid pretreatment is normally applied to improve the selectivity towards lignin during ozonation. This will increase the efficiency during ozone bleaching by removing the metal ions (Lachenal & Bokström, 1986; Roncero, Queral, Colom, & Vidal, 2010). After acidic pre-

* Corresponding author.
E-mail addresses: hrokiah@usm.my, hrokiah1@gmail.com (R. Hashim).

http://dx.doi.org/10.1016/j.carbpol.2016.09.053
0144-8617/

treatment, the native lignin can be converted to lignin derivative which is much easier to be removed during bleaching (Nimz & Berg, 1991). Water pre-hydrolysis and soda pulping were normally employed to aid in solubilizing the hemicelluloses fragments and increase the extractability of lignin during soda pulping. At this stage also, some carbonyl groups were removed from the hemicelluloses (Wan Rosli, Leh, Zainuddin, & Tanaka, 2003).

Oil palm trunk (OPT) consists mostly of parenchyma and vascular bundle that are rich in holocellulose ranging from 77% to 82%, and low in lignin content that is between 21% and 12% (Lamaming, Hashim, Leh, Sulaiman, & Sugimoto, 2015a), respectively. High in holocellulose and low in lignin content make OPT a good raw material for cellulose nanocrystal isolation.

With the rapid development research on cellulose nanocrystals, the main challenge is to find new source, new application as well as new preparation procedures. Our previous works successfully isolated the cellulose nanocrystals from oil palm trunk using sulfuric acid hydrolysis assisted by the chemo-mechanical treatment using sodium hypochlorite as a bleaching agent (Lamaming et al., 2015b, 2015c). The method proved to be effective in isolating the cellulose nanocrystals. However, the method used a chlorine-based bleaching agent with high concentrated acid. Therefore, the objective of this study is to improve the method of bleaching process in isolation of cellulose nanocrystals synthesis from oil palm trunk by using total chlorine free (TCF) by means of ozone bleaching followed by hydrochloric acid hydrolysis to increase the crystallinity properties of the cellulose nanocrystals.

2. Methods

2.1. Pre-water hydrolysis

Two types of cellulose nanocrystals were prepared from oil palm trunk with water pre-hydrolysis and without water pre-hydrolysis. The oil palm trunks were debarked and cut into chips of size of 2–5 cm before drying in an oven at a temperature 50 °C. Prior to pre-hydrolysis, the moisture content of the dried OPT fiber was calculated and the samples were subjected to water pre-hydrolysis by cooking the OPT in the digester for 2 h (1 h soaking time and 1 h cooking time) at 160 °C. Then the OPT fibers were washed and the moisture content was calculated before soda pulping was conducted.

2.2. Soda pulping pulp

The soda pulping followed the method by Wan Rosli et al. (2003) and Leh, Wan Rosli, Zainuddin, & Tanaka (2008). Both samples, with and without water pre-hydrolysis were subjected to soda pulping. The amount of cooking liquor was calculated and 25% alkali charge was used for the pulping processes based on the oven dry weight of raw material. The amount of sodium hydroxide solution and water needed were calculated based on the oven-dried weight of the sample to liquor ratio 1:7. The percentage of anthraquinone used was 0.1%. The samples were cooked for 3 h with 1 h to reach a temperature at 160 °C and followed by 2 h cooking time. The black-brown fibers were then washed in a hydrapulper to wash the pulp from black liquor for 10 min and the moisture content was measured.

2.3. Ozone bleaching and preparation of purified cellulose

Ozone bleaching was conducted following the method described by Lai (2011). Prior to ozone bleaching, the pulps were treated by soaking in sulfuric acid to increase the selectivity towards lignin in the ozone stage. About 15 g of oven dry weight (OD) pulp was acidified to the target of pH 1.5 which was adjusted by an addition of sulfuric acid and were soaked for 30 min before being pressed into a consistency of 25%. Ozone bleaching was carried out in a stainless steel reactor equipped with a motor stirrer and connected to an ozone generator (Ozone Solutions) and an oxygen cylinder. The acid pre-treated pulp was then placed into the ozone chamber, secured tightly and the ozone was run for 1 min and 10 min reaction time. After 11 min of total time, the unreacted ozone was released from the chamber for 20 min. After the ozone bleaching process had ended, the white pulp was washed thoroughly with distilled water. The resulting cellulose was then soaked in 6% potassium hydroxide (KOH) at 20 °C for 24 h. The purified cellulose were then washed until neutral and stored in a sealed vinyl plastic in the refrigerator.

2.4. Isolation of cellulose nanocrystals

Isolation of cellulose nanocrystal was done with acid hydrolysis following Nair and Dufresne (2003). The purified cellulose was hydrolyzed with 3N hydrochloric acid at 80 °C for 90 min under stirring. The suspension was then diluted with deionized water before being placed in the dialysis tube in distilled water until it is free from acid. The cellulose nanocrystals obtained were then dispersed in the sonicator for 5 min and stored in the refrigerator for future use.

2.5. Characterization

2.5.1. Chemical composition analysis

The preparation of samples for chemical analysis was done according to TAPPI (1997) with the ethanol-toluene ratio of 2:1. Lignin content was examined according to TAPPI 222 om-02 (TAPPI, 2002). The holocellulose content was performed following Wise, Murphy, and D'Addieco, 1946. Cellulose content was done by removing hemicellulose from the holocellulose with 17.5% sodium hydroxide. All the measurement was done in triplicate.

2.5.2. Scanning electron microscopy

The morphological properties of the fibers of unbleached and bleached pulp with water and without water pre-hydrolysis were viewed by an LEO Supra 50 Vp field emission scanning microscope (FESEM) with ultra-high resolution. All samples were coated with gold using sputter coater model Polaron SC 515 ± 20 nm to avoid charging and to improve the quality of the SEM micrographs.

2.5.3. Transmission electron microscopy

A drop of the sonicated cellulose nanocrystals suspension (0.01% of w/v) was deposited onto the carbon-coated TEM grid. The excess liquid was absorbed by filter paper before staining and allowed to dry. The completely dried specimen, then were viewed in a Philips CM12 electron microscope with Docu Version 3.2 image analysis. A total of 30 fibers was measured for their diameter and length directly from the TEM micrographs with the Image Tools software (Rosa, Rehman, de Miranda, Nachtigall, & Bica, 2012).

2.5.4. Fourier transform infrared (FTIR) spectroscopy

The FTIR spectra of the fibers before and after bleaching, and cellulose nanocrystals obtained were recorded in a transmission mode between wavenumbers of 4000 cm^{-1} and 500 cm^{-1} by using pellets. The pellets were prepared by finely grounding 5 mg of the samples in a matrix of 95 mg KBr followed by compression to form a pellet about 1 mm thick. Thermo Scientific model Nicolet iS10 spectrometer machine was used to collect the spectrum under infrared light.

2.5.5. Thermogravimetric analysis

Thermogravimetric analysis (TGA) was carried out on Mettler Toledo TGA/DSC 1 Star^e System instrument. All samples were

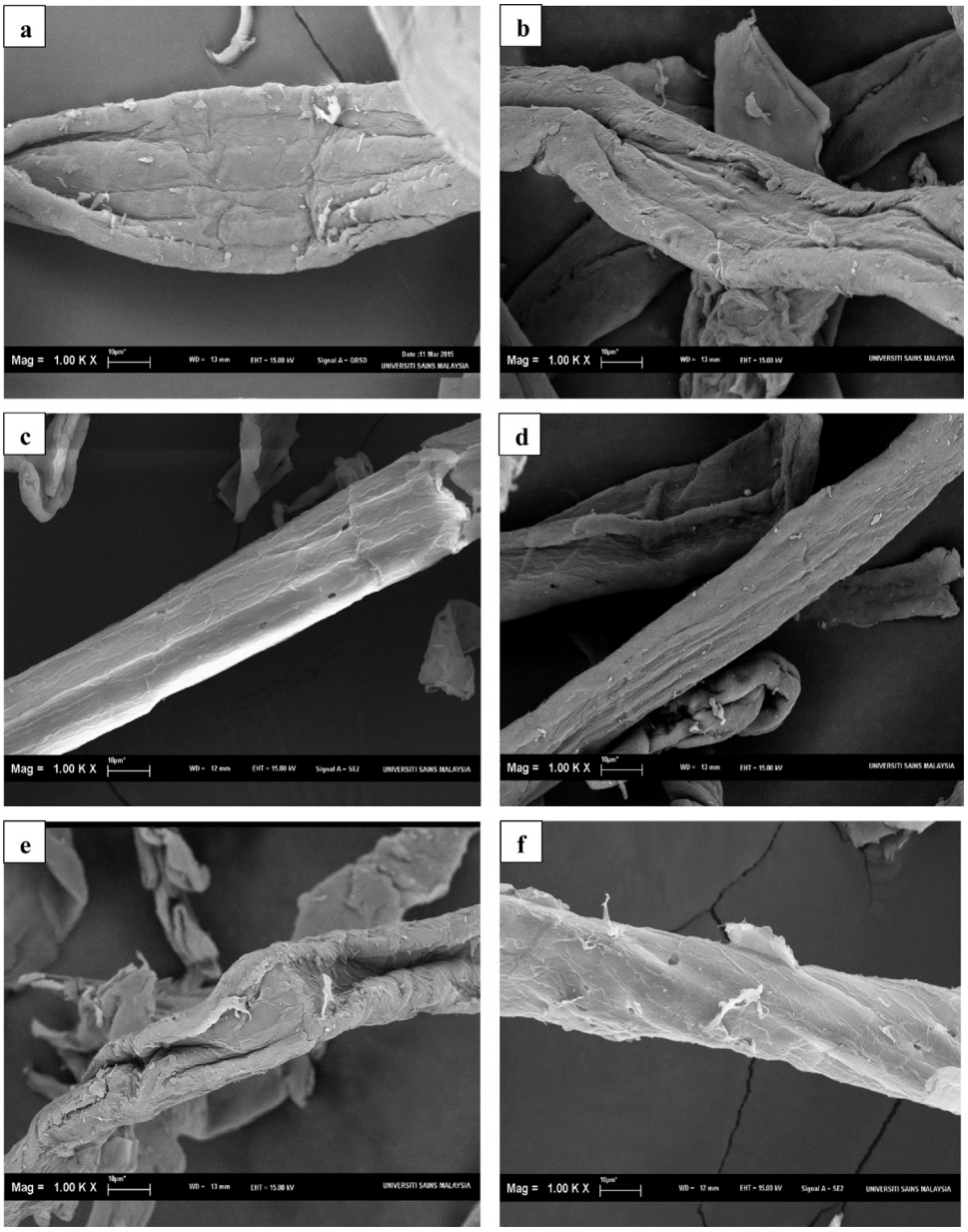

Fig. 1. SEM micrographs of oil palm trunk fibers without pre-hydrolysis; (a) unbleached pulp after soda pulping (b) ozone bleached cellulose (c) purified cellulose after acid hydrolysis; and with pre-hydrolysis (d) unbleached pulp after soda pulping (e) ozone bleached cellulose (f) purified cellulose after acid hydrolysis.

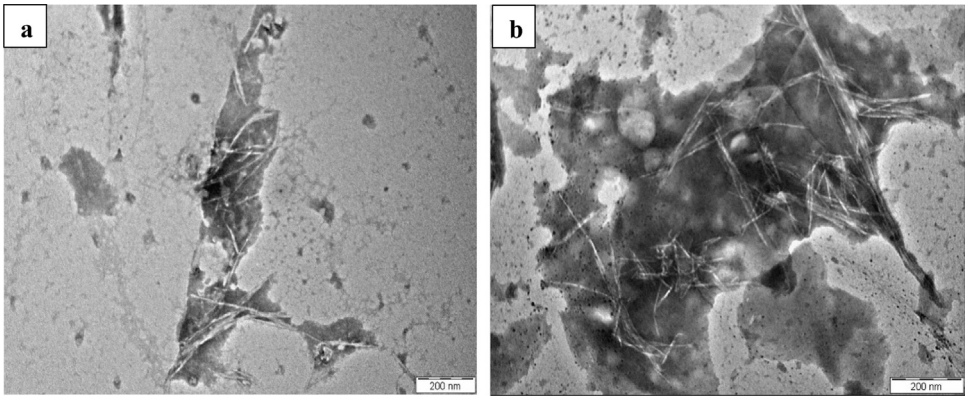

Fig. 2. TEM micrographs of the cellulose nanocrystals of oil palm trunk (a) without pre-hydrolysis and (b) with pre-hydrolysis.

scanned from 30 to 800 °C at a heating rate of 10 °C min^{-1} with nitrogen as purge gas at a flow rate 110 mL min^{-1}.

2.5.6. X-ray diffraction analysis

The X-ray diffractometer with CuKα radiation (wavelength of 1.5406 Å) generated at operating voltage and current of 40 kV and 30 mA was used to collect all the diffractograms of all samples. The CuKα radiation was filtered electronically with a Ni-filter. The intensities were collected at a 2θ angle range from 5° to 50° in reflection mode scanned at 2°/min. The crystallinity index was calculated according to Segal method (Segal, Creely, Martin, & Conrad, 1959).

3. Results and discussion

3.1. Chemical composition analysis

The chemical compositions of oil palm trunk with and without pre-hydrolysis were depicted in Table 1. Generally, the lignin contents of all fibers were observed below 0.5%. The ozone bleached cellulose with pre-hydrolysis showing an absence of lignin after ozone bleaching applied to the pulp. It is said that the water pre-hydrolysis facilitated the delignification rate during soda pulping by destroying or degrading the hemicelluloses to alkali-soluble substances (Wan Rosli et al., 2003). The holocellulose contents after soda pulping of fibers with and without water pre-hydrolysis were 93.7% and 98.4%, respectively. The value increased by means 1–2% after ozone bleaching. It appears that the alpha cellulose content showed a reduction in value after ozonation from 82.2% to 74.7% (pulp without pre-hydrolysis) and from 85.1 to 78.2% (pulp with pre-hydrolysis), respectively. The decrease varied between 7 and 8% was observed in the value of α-cellulose content and was expected since the cellulose will degrade during the ozone bleaching.

3.2. Morphological study

Fig. 1 displays the micrographs of oil palm trunk fibers with and without pre-hydrolysis after soda pulping, ozone bleaching and acid hydrolysis. After the soda pulping, the fibers without pre-hydrolysis showed rougher surface with impurities on the surface (Fig. 1a) and with ozonation, the surface of the fibers seem to be rougher (Fig. 1b). The fibers are smooth, sleek and clean showing no fibrillation as can be seen in Fig. 1c showing the removal of impurities or organic materials that were dissolved during acid hydrolysis.

On the other hand, fibers with pre-hydrolysis (Fig. 1d and e) showed rougher and have a split in the surface of the fibers after soda pulping and ozone bleaching. Fig. 1f showed that on the surface of fibers with pre-hydrolysis appeared to be flayed or peeled (Roncero, Torres, Colom, & Vidal, 2003). It can be observed that the peeled rough surface of fibers that underwent water pre-hydrolysis was improved and facilitated fibrillation during pulping and bleaching process. It also made the fibers susceptible to attack by the hydrochloric acid towards the interior region of the fibers which is the area of amorphous region.

3.3. Transmission electron microscopy (TEM)

The TEM micrographs of cellulose nanocrystals isolated from oil palm trunk with and without pre-hydrolysis are shown in Fig. 2a and b. Individualization of rod-like for both cellulose nanocrystals can be observed. The diameter and length of individual cellulose nanocrystals with pre-hydrolysis are about 3.58 nm and 82.81 nm (aspect ratio of 23) showing smaller in length when compared to cellulose nanocrystals without pre-hydrolysis that are 7.68 nm and 361.81 nm (aspect ratio of 47), respectively. The size of the nanocrystals isolated in this study was much smaller when compared with that of our previous study (Lamaming et al., 2015b, 2015c). The dimensions are also comparable to those cellulose whiskers (also known as cellulose nanocrystals) isolated from rice husk using TCF method of two-step bleaching done by Rosa et al. (2012). The dimensions of cellulose nanocrystals of OPT showed shorter diameter but longer in length than the rice husk. The difference in the aspect ratios (length over diameter) could be attributed to the water pre-hydrolysis that was applied to the fibers. The water pre-hydrolysis removed some of the hemicelluloses and softens the fibers that provided a good accessibility of the chemicals to react during pulping and bleaching.

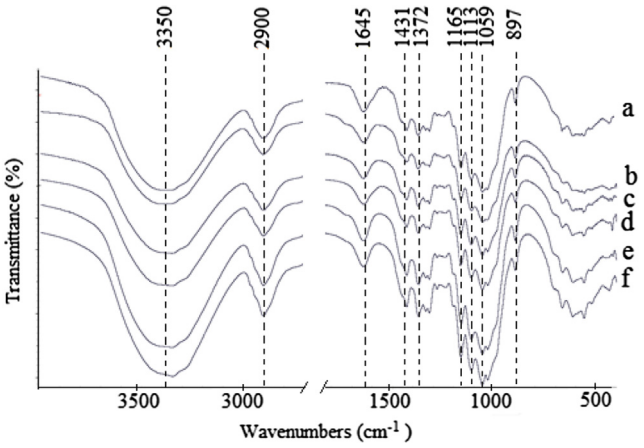

Fig. 3. FTIR spectra using a break abscissa in the 500–1800 cm^{-1} and 2800–4000 cm^{-1} region of oil palm trunk fibers without pre-hydrolysis; (a) unbleached pulp after soda pulping (b) ozone bleached cellulose (c) cellulose nanocrystals; and with pre-hydrolysis (d) unbleached pulp after soda pulping (e) ozone bleached cellulose (f) cellulose nanocrystals.

3.4. Fourier transform infrared spectroscopy

Changes in functional group that occurred in the fibers with and without water pre-hydrolysis were examined using a break abscissa in the FTIR spectra. Fig. 3 exhibits the FTIR spectra of fibers with and without water pre-hydrolysis after soda pulping, ozone bleaching and cellulose nanocrystals form. Generally, the spectra pattern looks similar. The difference could only be seen in the broadening or increasing in the intensity of the peaks. Peaks around 3400 cm^{-1} were attributed to the OH band where the inter-chain hydrogen bonds involving the C6 position (primary hydroxyl groups) resulted in the formation of crystalline regions (Ilharco, Garcia, lopes da Silva, & Viera Ferreira, 1997). It is worth noting the fact that the maximum wavenumber for the OH stretching band is below 3400 cm^{-1} is a good indication that the crystalline domains in all samples have lattice type 1 (Ilharco et al., 1997).

The peaks at 1372 cm^{-1}, 1375 cm^{-1} and 1316 cm^{-1} occur due to COH and HCC bending vibrations with peaks 1372 cm^{-1} and 1335 cm^{-1} represent the typical crystalline cellulose peaks (Garside & Wyeth, 2003). Peak at 1430 cm^{-1} was assigned as crystalline whilst peak at 897 cm^{-1} was assigned as amorphous. If the peak at 1430 cm^{-1} and 1111 cm^{-1} was not detected in the spectra, it indicated the absence of crystalline cellulose I type (Colom & Carillo, 2002).

The amount of the crystallinity of cellulose presence in the fibers also can be detected at the peak 1280 cm^{-1}, assigned to the CH bending which is a typical band for crystalline cellulose (Ilharco et al., 1997). The presence of the peak shows an increasing amount of crystalline cellulose. In some spectra (c and f), the

Table 1
Chemical composition of oil palm trunk fibers.

Fibers	Lignin (%)	Holocellulose (%)	α-cellulose (%)
Unbleached pulp without pre-hydrolysis	0.48 ± 0.11	93.69 ± 0.22	82.17 ± 1.13
Ozone bleached cellulose without pre-hydrolysis	0.38 ± 0.25	95.23 ± 0.47	74.73 ± 1.38
Unbleached pulp with pre-hydrolysis	0.27 ± 0.14	98.42 ± 0.14	85.14 ± 1.44
Ozone bleached cellulose with pre-hydrolysis	None	99.61 ± 0.30	78.22 ± 1.24

Table 2
Thermal properties of different type of fibers from oil palm trunk after several treatment.

Fibers	Onset Temperature (°C)	DTG peak (°C) T_{max}	Residue at 800 °C (%)
Unbleached pulp without pre-hydrolysis	307.96	356.29	10.37
Ozone bleached cellulose without pre-hydrolysis	311.43	337.75	7.60
Cellulose nanocrystals without pre-hydrolysis	322.54	345.13	5.88
Unbleached pulp with pre-hydrolysis	320.08	357.62	8.55
Ozone bleached cellulose with pre-hydrolysis	318.32	345.72	7.09
Cellulose nanocrystals with pre-hydrolysis	323.53	341.37	2.33

peak at 1280 cm^{-1} which is due to the CH_2 vibrations was relatively intense while in others it was relatively weak as almost absent. This is due to the acid hydrochloric attacking the amorphous region during acid hydrolysis thus increase the intensity of the peaks (Kavkler, Gunde-Cimerman, Zalar, & Demšar, 2011).

Reduction of the peaks at 900 cm^{-1} indicates the amorphous characteristics of cellulose. Broadening of the peak shows a larger amount of amorphous structure. Since all the peaks observed are sharp, it indicates less amorphous regions in the sample that was being examined. The absorbance tends to increase when pre-hydrolysis with water was employed to the fibers.

3.5. Thermal analysis

Fig. 4 exhibits the results of the TGA analysis. Fig. 4a depicted the weight loss percentage curves as a function of temperature while Fig. 4b gives the DTG derivative curves of all samples. Generally, if the polymeric portion of a material is relatively stable, only low molecular mass component will be lost below 300 °C in nitrogen gas. Then, a polymer will degrade and volatilize in temperature between 300 and 600 °C. Basically, all TGA curves illustrated two stages of weight loss processes. The first stage of thermal degradation occurred between 30 and 150 °C, showing the range of the initial weight loss of below 10% where the evaporation of the absorbed water occurred. The second stage corresponds to thermal decomposition of cellulosic material took place between 200 and 400 °C.

Yang et al. (2006) concluded in their study that biomass decomposition occurred in four ranges which are moisture evolution (< 220 °C), hemicellulose decomposition (220–315 °C), cellulose decomposition (315 °C) and lignin decomposition (>400 °C). Above 600 °C, only inorganic compound that is stable enough to remain at this temperature (Bruce, Bair, Vyazovkin, Gallagher, & Riga, 2008). However, linear aromatic and other cyclic structure will not be completely converted to gaseous products when heated to 600 °C as it promotes char formation or degradation of carbonaceous structure in nitrogen (Bair, 1997).

The onset decomposition temperature of cellulose nanocrystals with and without pre-hydrolysis is higher compared to other fibers as can be seen in Table 2. This behavior is attributed to the high crystallinity index value calculated in these fibers. This value is agreeable as thermal decomposition of the cellulose shifted to higher temperature with the increasing of the crystallinity index as reported by Kim, Eom, and Wada, 2010. The same trend also has been reported by other researchers investigating with other raw materials that were Alfa fibers (Trache, Donnot, Khimeche, Benelmir, & Brosse, 2014) and wood (Chen et al., 2011). The crystalline regions of cellulose nanocrystals are expected to improve the thermal stability of the lignocellulosic fibers (Yang et al., 2006) and act as barriers for the heat transfer, which possibly increase the thermal stability of the cellulose (Poletto et al., 2014).

Table 3
Crystallinity index (%) values of different type of fibers.

Fibers	Crystallinity index (%)
Unbleached pulp without pre-hydrolysis	54.1
Ozone bleached cellulose without pre-hydrolysis	56.54
Cellulose nanocrystals without pre-hydrolysis	69.09
Unbleached pulp with pre-hydrolysis	60.89
Ozone bleached cellulose with pre-hydrolysis	63.94
Cellulose nanocrystals with pre-hydrolysis	74.81

From Table 2, the unbleached with and without pre-hydrolysis fibers had greater DTG curve peak temperature (T_{max}). If compared to the case of bleached pulp and cellulose nanocrystals, a decrease up to 19 °C can be observed. The reasonable explanation is that bleached cellulose fibers underwent ozone bleaching resulting in the cellulose degradation. On the other hand, cellulose nanocrystals that were subjected to the same process with the addition of acid hydrolysis tend to degrade more as the acid hydrolysis make the fibers more accessible to degrade when increasing the temperature. However, thermal decomposition of cellulose nanocrystals from oil palm trunk found in this study is higher in comparison to other part of oil palm (empty fruit bunch) as studied by Mohamad Haafiz, Eichhorn, Hassan, and Jawaid, 2013. The same thermal decomposition rate of 345° C for rice husk whisker was reported by Rosa et al. (2012) using different procedures of TCF method.

3.6. X-ray diffraction analysis

The integrity of the nanoparticle crystallinity was ascertained by conducting X-Ray diffraction analysis was conducted. Fig. 5 displays the typical XRD diffractograms pattern of cellulose I. According to Wada, Okano, & Sugiyama (2001), the crystallographic planes are differentiated according to the native cellulose structure where, peak at 2θ = 16.2°–16.3° reflection attributed to the (110) crystallographic plane. The amorphous phase was at the 2θ = 18.30°–18.40° and at 2θ = 21.9°–22.5°, the reflection was assigned to the (200) crystallographic plane of cellulose I (Wada et al., 2001; Popescu, Popescu, Lisa, & Sakata, 2011; Poletto, Zattera, Forte, & Santana, 2012). The X-ray diffraction patterns show an increasing trend of crystallinity and sharp diffraction peak at 2θ (22.5°) which indicates the crystallinity of the cellulose samples. From the Figure, it can be observed that no alteration in the XRD cellulose pattern suggesting that the reaction occurred predomi-

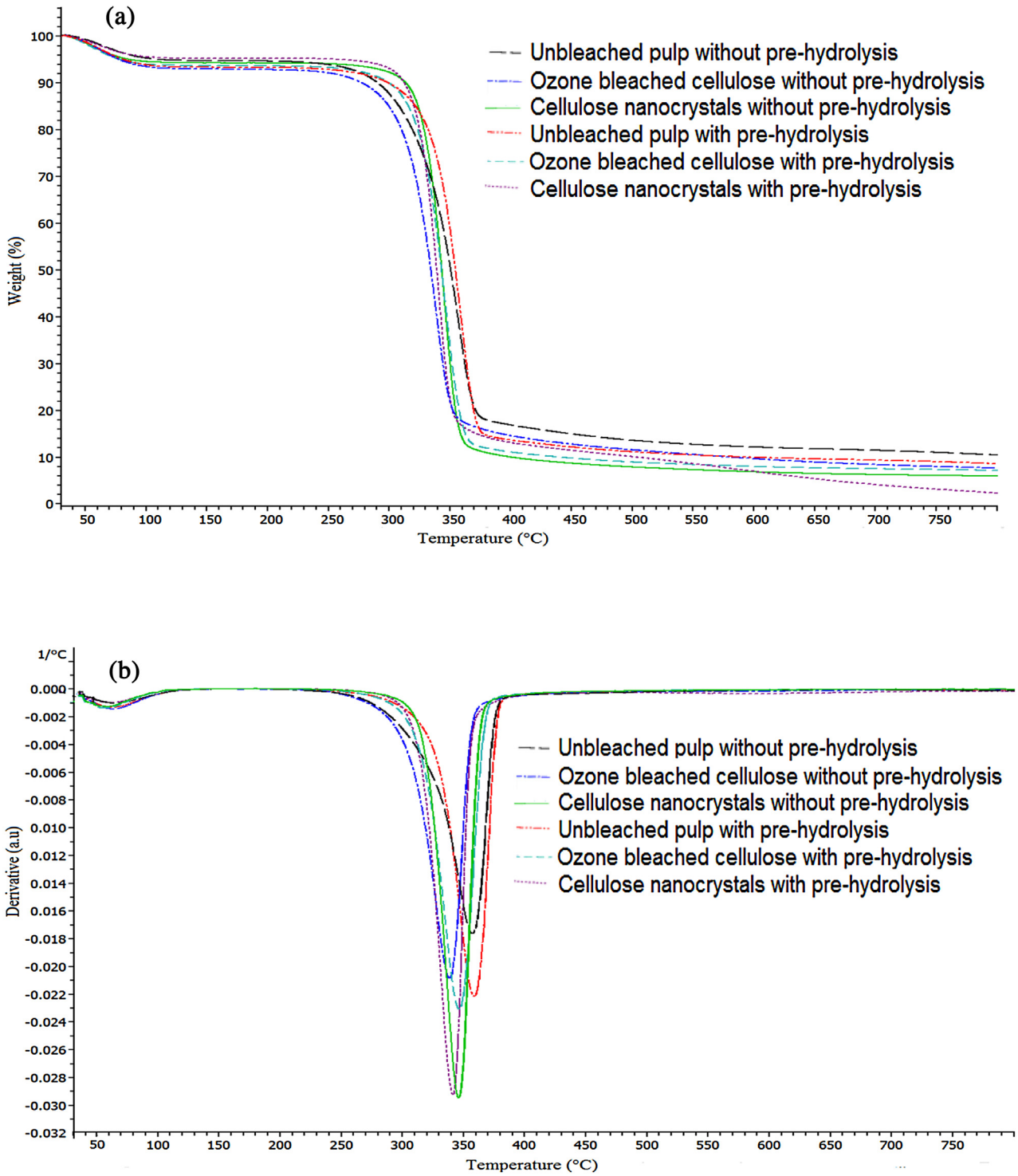

Fig. 4. Typical (a) TGA curves and (b) DTG curves for all fibers.

nantly on the surface without affecting in a great extent the internal structure of the material (Siqueira et al., 2013).

Table 3 displays the crystallinity index value of all fibers. It can be noted that the crystallinity index increased when the water pre-hydrolysis was applied to the fibers. The results showed that after ozone bleaching, fibers subjected to water pre-hydrolysis displayed a better crystallinity index value that is 63.94% compared to fibers without pre-hydrolysis 56.54%, showing an increase by 7%. Crystallinity values for fibers of bleached cellulose with pre-hydrolysis are in all cases higher than those for bleached cellulose without pre-hydrolysis, with a difference of 7% in unbleached pulp and in the cellulose bleached with the ozone. This indicates that fibers treated with the water pre-hydrolysis improved and helped the reactivity of the fibers with the ozone during the pulping and ozone bleaching.

Cellulose nanocrystals with pre-hydrolysis showed a 6% increase in the crystallinity index in comparison with the cellulose nanocrystals without pre-hydrolysis that is 74.81% to 69.09%. It can be observed that the crystallinity index in this study showed an increase of 5% and 10% in comparison to our previous studies (Lamaming et al., 2015b, 2015c), respectively. Therefore, bleach-

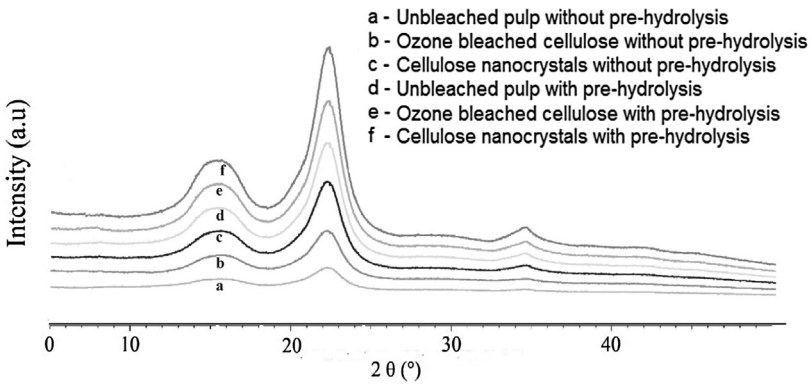

Fig. 5. XRD diffractograms for all fibers.

ing process increased the crystallinity of the unbleached pulp with and without pre-hydrolysis. It was also reported that ozone bleaching increased the degree of crystallinity by reducing the amorphous region (Roncero et al., 2003). When the amorphous domains of cellulose were attacked, chain scission and peeling reactions occurred and consequently the total amount of amorphous cellulose decreased while increasing the relative degree of crystallinity (Gümüskaya, Usta, & Kirei, 2003). When comparing the crystallinity index reported in this study with other part of the oil palm trunk, especially oil palm empty fruit bunch (OPEFB), the crystallinity index was lower compared to Mohamad Haafiz et al. (2013) that was 87%. However, the crystallinity of both cellulose nanocrystals from OPT in this study is higher in comparison to cellulose from rice husk (67%) reported by Rosa et al. (2012) when using different chlorine-free extraction method in isolating the cellulose nanowhiskers.

4. Conclusions

Cellulose nanocrystals were successfully isolated from oil palm trunk with and without pre-hydrolysis using soda pulping followed by ozone bleaching and hydrochloric acid hydrolysis. In this study, the isolation of cellulose nanocrystals from OPT using TCF method was shown to be efficient and effective. The SEM micrographs showed that fibers with pre-hydrolysis having a fibrillation and peeled on the surface of the fibers after acid hydrolysis process. Cellulose nanocrystals with 3–8 nm in width and 82–362 nm in length were obtained. Thermal stability data demonstrated that both cellulose nanocrystals having an improved thermal properties associated with an increasing crystallinity index value. The relative crystallinity of the cellulose nanocrystals reached approximately 75% for cellulose nanocrystals with water pre-hydrolysis. It can be concluded that the obtained results for both cellulose nanocrystals from oil palm trunk has a great potential to be applied in many industries such as pharmaceutical, food, medical as well as nanocomposites.

Acknowledgements

The authors would like to thank Ministry of Higher Education, Malaysia for the financial support (Ph.D fellowship of Junidah Lamaming), and Universiti Sains Malaysia for the project financial under a research grant (1001/PTEKIND/811255).

References

Bair, H. E. (1997). E. A. Turi (Ed.), *Thermal characterization of polymeric materials* (vol. 2) (2nd ed., vol. 2, pp. 2263–2420). San Diego: Academic Press.

Brinchi, L., Cotana, F., Fortunati, E., & Kenny, J. M. (2013). Production of nanocrystalline cellulose from lignocellulose biomass: Technology and applications. *Carbohydrate Polymers*, *94*, 154–169.

Bruce, P. R., Bair, H. E., Vyazovkin, S., Gallagher, P. K., & Riga, A. (2008). Thermogravimetric analysis (TGA). In J. D. Menczel, & R. B. Prime (Eds.), *Thermal analysis of polymers: Fundamentals and applications* (pp. 241–317). Hoboken, NJ, USA: John Wiley & Sons Inc.

Chandra, S., & Gratzl, J. S. (1985). Kinetics of carbohydrate and lignin degradation and formation of carbonyl and carboxyl groups in low consistency ozonation of softwood pulps. In *In proceedings of the international pulp bleaching conference* , pp. 27–35.

Chen, W., Yu, H., Liu, Y., Chen, P., Zhang, M., & Hai, Y. (2011). Individualization of cellulose nanofibers from wood using high-intensity ultrasonication combined with chemical pretreatments. *Carbohydrate Polymers*, *83*, 1804–1811.

Colom, X., & Carillo, F. (2002). Crystallinity changes in lyocell and viscose-type fibres by caustic treatment. *European Polymer Journal*, *38*, 2225–2230.

Durán, N., Lemes, A. P., Durán, M., Freer, J., & Baeza, J. (2011). A minireview of cellulose nanocrystals and its potential integration as co-products in bioethanol production. *Journal of the Chilean Chemical Society*, *56*(2), 672–677.

Eichhorn, S. J., Dufresne, A., Aranguren, M., Marcovich, N. E., Capadona, J. R., Rowan, S. J., et al. (2010). Review: Current international research into cellulose nanofibers and nanocomposites. *Journal of Material Science*, *45*, 1–33.

Eichhorn, S. J. (2011). Cellulose nanowhiskers: Promising materials from advanced applications. *Soft Matter*, *7*, 303–315.

Gümüskaya, E., Usta, M., & Kirei, H. (2003). The effects of various pulping conditions on crystalline structure of cellulose in cotton linters. *Polymer Degradation and Stability*, *81*, 559–564.

Garside, P., & Wyeth, P. (2003). Identification of cellulosic fibres by FTIR spectroscopy: Thread and single fibre analysis by attenuated total reflectance. *Studies in Conversation*, *48*(4), 269–275.

Habibi, Y., Lucia, L. A., & Rojas, O. J. (2010). Cellulose nanocrystals: Chemistry: self-assembling and applications. *Chemical Reviews*, *110*, 3479–3500.

Ilharco, L. M., Garcia, A. R., lopes da Silva, J., & Viera Ferreira, L. F. (1997). Infrared approach to the study of adsorption on cellulose: Influence of cellulose crystallinity on the adsorption of benzophenone. *Langmuir*, *13*, 4120–4132.

Kavkler, K., Gunde-Cimerman, N., Zalar, P., & Demšar, A. (2011). FTIR spectroscopy of biodegraded historical textiles. *Polymer Degradation and Stability*, *96*, 574–580.

Kim, U.-J., Eom, S. H., & Wada, M. (2010). Thermal decomposition of native cellulose: Influence on crystallite size. *Polymer Degradation and Stability*, *95*, 778–781.

Lachenal, D., & Bokström, M. (1986). Improvement of ozone prebleaching of kraft pulp. *Journal of Pulp and Paper Science*, *12*(2), 50–53.

Lai, W. J. (2011). *The effect of pH retention time and acid prewashing of ozone bleaching on kenaf soda-anthraquinone pulp Master dissertation*. Malaysia: School of Industrial Technology, Universiti Sains Malaysia., pp. 72.

Lamaming, J., Hashim, R., Leh, C. P., Sulaiman, O., & Sugimoto, T. (2015). Chemical, crystallinity and morphological properties of oil palm trunk parenchyma and vascular bundle. *International Journal of Environmental Engineering*, *2*(1), 66–70.

Lamaming, J., Hashim, R., Sulaiman, O., Leh, C. P., Sugimoto, T., & Nordin, N. A. (2015). Cellulose nanocrystals isolated from oil palm trunk. *Carbohydrate Polymers*, *127*, 202–208.

Lamaming, J., Hashim, R., Sulaiman, O., Leh, C. P., Sugimoto, T., & Nasir, M. (2015). Isolation and characterization of cellulose nanocrystals from parenchyma and vascular bundle of oil palm trunk (Elaeis Guineensis). *Carbohydrate Polymers*, *134*, 534–540.

Lavoine, N., Desloges, I., Dufresne, A., & Bras, J. (2012). Microfibrillated cellulose-Its barrier properties and applications in cellulosic materials: A review. *Carbohydrate Polymers*, *90*, 735–764.

Leh, C. P., Wan Rosli, W. D., Zainuddin, Z., & Tanaka, R. (2008). Optimization of oxygen delignification in production of totally chlorine-free cellulose pulps from oil palm empty fruit bunch fiber. *Industrial Crop and Product*, *28*, 260–267.

Mohamad Haafiz, M. K., Eichhorn, S. J., Hassan, A., & Jawaid, M. (2013). Isolation and characterization of microcrystalline cellulose from oil palm biomass residue. *Carbohydrate Polymers*, *93*, 628–634.
Nair, K. G., & Dufresne, A. (2003). Crab shell chitin whisker reinforced natural rubber nanocomposites.1: Processing and swelling behavior. *Biomacromolecules*, *4*, 657–665.
Nimz, H. H., A. Berg, A., 1991. Lignin removal method using ozone and acetic acid. United States Patent, 5 074 960. Acetocell GmbH & Co. KG, Hamburg, Germany.
Poletto, M., Zattera, A. J., Forte, M. M. C., & Santana, R. M. C. (2012). Thermal decomposition of wood components and cellulose crystallite size. *Bioresource Technology*, *109*, 148–153.
Poletto, M., Ornaghi, H. L., Jr., & Zattera, A. J. (2014). Native cellulose: Structure: characterization and thermal properties. *Materials*, *7*, 6105–6119.
Popescu, M. C., Popescu, C. M., Lisa, G., & Sakata, Y. (2011). Evaluation of morphological and chemical aspects of different wood species by spectroscopy and thermal methods. *Journal of Molecular Structure*, *988*, 65–72.
Pouyet, F., Chirat, C., Potthast, A., & Lachenal, D. (2014). Formation of carbonyl groups on cellulose during ozone treatment of pulp: Consequences for pulp bleaching. *Carbohydrate Polymers*, *109*, 85–91.
Ragnar, M., Eriksson, T., & Reitberger, T. (1999). Radical formation in ozone reactions with lignin and carbohydrate model compounds. *Holzforschung*, *53*, 292–298.
Roncero, M. B., Torres, A. L., Colom, J. F., & Vidal, T. (2003). TCF bleaching of wheat straw pulp using ozone and xylanese.Part A: Paper quality assessment. *Bioresource Technology*, *87*, 305–314.
Roncero, M. B., Queral, M. A., Colom, J. F., & Vidal, T. (2010). Why acid pH increases the selectivity of the ozone bleaching processes. *Ozone: Science and Engineering*, *25*(6), 523–534.
Rosa, S. M. L., Rehman, N., de Miranda, M. I. G., Nachtigall, S. M. B., & Bica, C. I. D. (2012). Chlorine-free extraction of cellulose from rice husk and whisker isolation. *Carbohydrate Polymers*, *87*, 1131–1138.
Segal, L., Creely, J. J., Martin, A. E., & Conrad, C. M. (1959). An empirical method for estimating the degree of crystallinity of native cellulose using the X-Ray diffractometer. *Textile Research Journal*, *29*, 786–794.
Shatalov, A. A., & Pereira, H. (2007). Polysaccharide degradation during ozone-based TCF bleaching of non-wood organosolv pulps. *Carbohydrate Polymers*, *67*, 275–281.
Shatalov, A. A., & Pereira, H. (2008). Arundo donax L. reed: New perspectives for pulping and bleaching. 5. Ozone-based TCF bleaching of organosolv pulps. *Bioresource Technology*, *99*(3), 472–478.
Simões, R., & Castro, J. (2001). Ozone depolymerization of polysaccharides in different materials. *Journal of Pulp and Paper Science*, *27*(3), 82–87.
Siqueira, G., Bras, J., Follain, N., Belbekhouche, S., Marais, S., & Dufresne, A. (2013). Thermal and mechanical properties of bio-nanocomposites reinforced by Luffa cylindrica cellulose nanocrystals. *Carbohydrate Polymers*, *91*, 711–717.
TAPPI Test Method. (1997). *Tappi T 264 cm-97 Preparation of wood for chemical analysis*. Technology Park Atlanta: TAPPI Press.
TAPPI Test Method. (2002). *Tappi T 222 om-02 Acid-insoluble lignin in wood and pulp*. Technology Park Atlanta: TAPPI Press.
Trache, D., Donnot, A., Khimeche, K., Benelmir, R., & Brosse, N. (2014). Physico-cehmical properties and thermal stability of microcrystalline cellulose isolated from Alfa fibers. *Carbohydrate Polymers*, *104*, 223–230.
Wada, M., Okano, T., & Sugiyama, J. (2001). Allomorphs of native crystalline cellulose I evaluated by two equatorial d-spacings. *Journal of Wood Science*, *47*, 124–128.
Wan Rosli, W. D., Leh, C. P., Zainuddin, Z., & Tanaka, R. (2003). Optimising of soda pulping variables for preparation of dissolving pulps from oil palm fibre. *Holzforschung*, *57*, 106–114.
Wise, L. E., Murphy, M., & D'Addieco, A. A. (1946). Chlorite holocellulose, its fractionation and bearing on summative wood analysis and on studies or on hemicelluloses. *Paper Trade Journal*, *122*(2), 35–42.
Yang, H., Yan, R., Chen, H., Zheng, C., Lee, D. H., & Liang, D. T. (2006). In-Depth investigation of biomass pyrolysis based on three major components: Hemicellulose cellulose and lignin. *Energy and Fuels*, *20*, 388–393.